

# Preparation, Characterization and Electrochemical Sensing Property of Poly (2-methoxyaniline) Microspheres

R. Suresh<sup>1</sup>, K. Giribabu<sup>2</sup>, R. Manigandan<sup>2</sup>, S. Praveen Kumar<sup>2</sup>, S. Munusamy<sup>2</sup>,  
S. Muthamizh<sup>2</sup>, A. Stephen<sup>3</sup>, V. Narayanan<sup>2\*</sup>

Department of Chemistry, SRM University, Ramapuram, Chennai, India<sup>1</sup>

Department of Inorganic Chemistry, University of Madras, Guindy Campus, Chennai, India<sup>2</sup>

Department of Nuclear Physics, University of Madras, Guindy Campus, Chennai, India<sup>3</sup>

\*Corresponding author

**ABSTRACT:** Poly(2-methoxyaniline) microspheres (P2MA) were prepared by oxidative polymerization method using potassium persulphate and  $\beta$ -naphthalenesulphonic acid (NSA) as an oxidizing agent and dopant respectively. The spectral, morphological, and electrochemical characteristics of P2MA microspheres were determined from the results of Fourier transform infrared (FTIR) spectroscopy, Raman spectroscopy, UV-Vis spectroscopy, scanning electron microscopy (SEM) and cyclic voltammetry (CV). The electrochemical sensing property of P2MA microspheres were studied by CV and chronoamperometry (CA) using uric acid (UA) as an analyte. The calibration curve for UA was obtained over the range of 6.6 to 62.5  $\mu$ M with corresponding sensitivity of 0.003  $\mu$ A $\mu$ M<sup>-1</sup>. The proposed sensor is simple, easy and cost effective which will have a great potential in electrochemical biosensor.

**KEYWORDS:** Poly(2-methoxyaniline), microspheres, electrochemistry, sensor, uric acid.

## I. INTRODUCTION

Conducting polymers are found to be new class of materials because of their unique electrical and optical properties. They are widely used in rechargeable batteries, chemically modified electrodes, sensors, gas separation membranes, light emitting diodes, electrochromic and electronic devices [1-5]. By proper doping, the conductivity of these polymers can be varied from semiconducting to metallic conducting [6]. The concept of doping in the conducting polymer is unique in its process, type and mechanistic point of view. A relatively small quantity of a chemical substance (dopant) changes the electrical conductivity of the non-conducting or very low conducting polymer to a semiconducting or metallic conducting polymer. Doping is a fully reversible process that occurs without any degradation of polymer. In conjugated polymer generally redox doping is used i.e. electron donation to a  $\pi$ -conjugated system (n-type) or electron withdrawal from a  $\pi$ -conjugated system (p-type). In case of conducting polymer like polyaniline (PANI) and its derivatives the redox as well as neutral doping was applicable for that purpose. The neutral doping is one which does not donate or take up electron from the  $\pi$ -conjugated polymer. In fact such neutral dopants show more importance in case of polyaniline and its derivatives over redox dopants due to easy doping procedure, good reproducibility and reversibility and better conductivity. Different organic and inorganic acids are used as neutral dopant in conducting polyaniline and its derivatives. In situ acid doping occurs if polyaniline or its derivatives are synthesized in acid medium. Among conducting polymers, PANI is one of the most studied conducting polymers due to its good conductivity, stability, highly colored material, easy and low cost of production. PANI exist in three forms namely fully reduced leucoemeraldine, half oxidized emeraldine and fully oxidized pernigraniline. PANI can be synthesized by chemical or electrochemical method. Eventhough the electrochemical method has the advantages like high purity; the chemical method is preferred because it can be prepared in large scale which is attractive from a

**International Journal of Innovative Research in Science, Engineering and Technology**

An ISO 3297: 2007 Certified Organization

Volume 4, Special Issue 1, February 2015

**THIRD NATIONAL CONFERENCE ON ADVANCES IN CHEMISTRY (NCAC – 2015)**On 18<sup>th</sup> February 2015

Organized by

Department of Chemistry, Easwari Engineering College (SRM Group of Institutions), Chennai-600089, India.

practical point of view. PANI has many great applications in various fields including sensors, electrochromic devices, batteries, anticorrosion and electronic devices [7]. However, one disadvantage of PANI is its poor processability. PANI itself is not soluble in most common solvents and decomposes before it melts. In order to improve its processability, few reports show that the complexation of PANI with sulphonic acids [8]. Another method to improve the processability of PANI is to use of PANI derivatives. For instance, poly(2,5-dimethoxyaniline) [9], polymethylaniline [10] and polyanthranilic acid [11]. It is believed that the substituent in PANI chain decrease the stiffness of the polymer making it easier to dissolve. In this paper we have reported the preparation of P2MA microspheres by chemical method. The prepared microspheres were characterized by FTIR, Raman, UV-Vis spectroscopy, SEM and CV. Further, the UA sensing property of the prepared P2MA microspheres was evaluated by CV and CA. The results suggest that the P2MA microspheres can be used as electrochemical biosensor.

## II. EXPERIMENTAL

2-methoxyaniline, potassium persulfate, and  $\beta$ -naphthalenesulphonic acid were purchased from Qualigens. 2-methoxyaniline was distilled under reduced pressure prior to use. Doubly distilled (DD) water was used as the solvent throughout the experiments.

### Preparation of P2MA microspheres

Typical synthetic procedure is as follows: Poly(2-methoxyaniline) microspheres were synthesized by chemical oxidation of 2-methoxyaniline. In 250 mL round bottom flask, 0.56 mL of 2-methoxyaniline and the required amount of NSA were dissolved in DD water. The above solution was cooled in a refrigerator at 5 °C for 30 min and then a pre-cooled aqueous solution of potassium persulphate as an oxidant was added drop wisely. The molar ratio of oxidant to 2-methoxyaniline in the final solution was 1:1. The reaction is continued for 24 h during which the precipitation of black colored P2MA microspheres were formed. The obtained sample was filtered and washed with water and acetone three times. The final product was dried in vacuum at room temperature for 24 h.

### Characterization techniques

FT-IR spectrum was recorded on Shimadzu FT-IR 8300 series instrument by using potassium bromide pellets. Raman spectrum was recorded by using laser Raman microscope, Raman-11 Nanophoton Corporation, Japan. The UV-Visible spectrum of P2MA microspheres was recorded on UV-1601OC, Shimadzu instrument using absolute ethanol as solvent. The morphology of the polymer was analyzed by FE-SEM using a HITACHI SU6600 field emission-scanning electron microscopy. The electrochemical experiments were performed on a CHI 1103A electrochemical instrument using the P2MA microspheres modified glassy carbon electrode (P2MA/GCE) and bare GCE as working electrode, a platinum wire was the counter electrode, and saturated calomel electrode (SCE) was the reference electrode.

### Fabrication of P2MA/GCE

The modifying process of the electrode was followed by drop coating method [12] and the procedure is as follows. Ultrasonication for 15 min was used to disperse 1 mg of P2MA microsphere into 5 mL of acetone to make homogeneous suspension. The highly polished GCE was coated with 5  $\mu$ L of the above suspension and dried in air. The modified electrode was activated in 0.1 M H<sub>2</sub>SO<sub>4</sub> solution by successive cyclic scans between 0.2 and +0.8 V. Before and after each experiment, modified electrode was washed with distilled water and reactivated by the method mentioned above.

## III. RESULT AND DISCUSSION

### FTIR analysis

The FT-IR spectrum of P2MA-NSA microspheres is shown in Fig. 1. The FTIR bands of P2MA-NSA microspheres are found at 1570, 1492, 1256, 1195, 1117, 1021, 951, 811, and 672 cm<sup>-1</sup>. The band at 1570 cm<sup>-1</sup> is assigned to C=C

ring stretching vibration. The bands at 1117 and 811  $\text{cm}^{-1}$  are due to the in-plane and out-of-plane C-H bending modes in 1,4-disubstituted benzene ring respectively. The band at 1492  $\text{cm}^{-1}$  is due to C-N stretching of the quinoid ring (Q), which arises on the protonation of P2MA by NSA. The bands position of P2MA-NSA has shifted to low-frequency than of emeraldine base, which indicate some changes in the benzenoid structure due to the polaron lattice. The doping of P2MA base by NSA leads to the formation of  $-\text{Q}=\text{N}+\text{H}-$  groups in the P2MA chain. The positive charge on the P2MA chain may lead to an increase in the dipole moment of the polymer that resulting in an increase in the intensity of the FT-IR bands [13]. Further, an intense band present at 951  $\text{cm}^{-1}$  is assigned to the ring-breathing mode of the quinoid group, which becomes active on protonation. In addition, the spectrum of P2MA-NSA exhibits new bands in the region of 1000 - 400  $\text{cm}^{-1}$  which are assigned to vibration of NSA. Particularly, a band at 610  $\text{cm}^{-1}$  is assigned to  $\text{SO}_3^-$  group of P2MA-NSA salt which confirms the doping of P2MA by NSA. These results are well consistent with previous report [14].

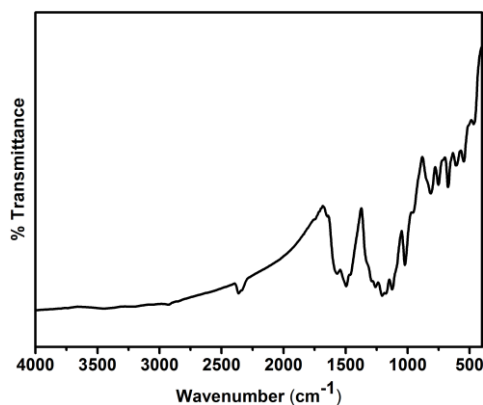


Fig. 1: FTIR spectrum of P2MA-NSA microspheres

#### Raman analysis

Raman spectrum of P2MA-NSA is shown in Fig. 2. The P2MA undergoes protonation of the amine nitrogen on doping with NSA, leading to the formation of  $\text{Q}=\text{N}+\text{H}$  species, which enhances conjugation in the P2MA chain. The high intensity peak at 1348  $\text{cm}^{-1}$  is related to the  $\text{C}=\text{N}^{+\bullet}$  stretching vibration [15]. The Raman bands at 1184 and 1652  $\text{cm}^{-1}$  are attributed to C-H in-plane bending and C-C stretching in the benzenoid ring respectively. Because of some difference in the conformation of the P2MA-NSA and the extent of doping of NSA, the frequency of C-C stretching vibration varies. The C-C bond is strengthened in the protonation-induced polaron lattice. The band at 1162  $\text{cm}^{-1}$  is to out-of-plane -CH bending of the polymer. The bands are observed at 1591 and 1532  $\text{cm}^{-1}$  are due to stretching vibration of the quinoid and benzenoid rings, respectively. It suggests a greater contribution of the quinoid structure to the bonding in the polymer salt. The former band has weak to medium intensity. Hence, it is clear that the synthesized P2MA-NSA is in the conducting state. Several less intense new bands also appear in Fig. 2 which corresponds to P2MA-NSA.

#### UV-Visible analysis

UV-Visible spectrum of P2MA-NSA is shown in Fig. 3. It shows a broad band at 316 and 550 nm. These absorption bands correspond to  $\pi-\pi^*$  and inter-ring charge transfer associated with excitation from benzenoid to quinoid moieties [16]. By comparing the UV-Visible spectrum of PANI with P2MA-NSA, the band for  $\pi-\pi^*$  transition is shifted to lower wavelength. This blue shift is due to the presence of  $-\text{OCH}_3$  group in the polymer. The Ginder et al.[17] have reported through their theoretical consideration that an increase in the dihedral angle or the ring torsion angle between adjacent aromatic rings of the polymer could cause a blue shift. A twist in the torsion angle is expected to increase the average band gap in the ensemble of the conjugated polymer system. Similarly Ghosh et al.[18] also reported a blue shift in the

case of poly(o-toluidine) due to the strong repulsion caused by the bulkier CH<sub>3</sub> group. This increases the torsion angle and decreases the valence width.

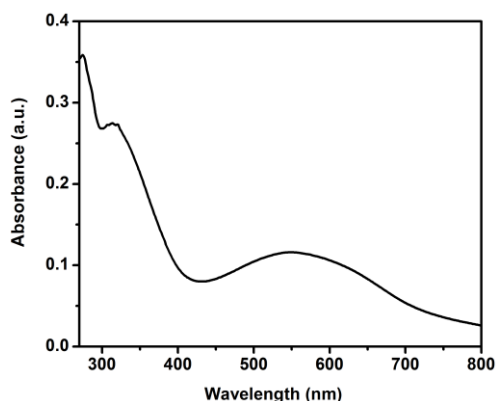


Fig. 3: UV-Vis spectrum of P2MA-NSA microspheres

#### SEM analysis

Fig. 4 shows SEM images of P2MA-NSA. It can be seen that the product showed a hollow spherical morphology with an opening at some point on the surface of the microspheres. The average outer diameter of the microspheres measured from SEM image is found to be ~2  $\mu$ m. It can be noted that the P2MA-NSA spheres with much smaller in size also found in the product.

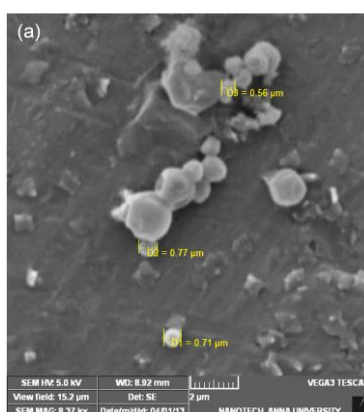


Fig. 4: SEM images of P2MA-NSA microspheres

#### Hollow spherical morphology and related formation mechanism

There are several mechanisms have been proposed for the formation of conducting polymer hollow spheres. In one of the mechanisms, self-assembled micelles form from the 2-methoxyaniline and NSA present during the initial stages of the reaction, and these micelles can act as soft templates (Scheme 2A) in the formation of the hollow spheres [19]. It is reasonable to expect that the NSA micelles can be form in our reaction system because of the presence of amphiphilic groups (-SO<sub>3</sub>H) and amphiphobic group (naphthalene ring) in NSA. 2-methoxyaniline exists in the form of both free 2-methoxyaniline monomer and 2-methoxyaniline cations, which are formed by acid–base reaction between NSA and 2-methoxyaniline. Positively charged 2-methoxyaniline cations can be attracted by anionic groups of NSA on the exterior of the micelles, while free 2-methoxyaniline can accumulate in the micelle hydrophobic interior,

and cause the original micelles to swell. These micelles composed of NSA and 2-methoxyaniline could be act as the templates for the formation of hollow spheres through a self-assembly process. When the potassium persulphate (oxidant) is added, the polymerization takes place at the water/micelle interface because of the hydrophilicity of potassium persulphate, followed by aggregation and fusion processes to form larger sized spheres as the nanospheres coalesce (Scheme 2B). With the progress of polymerization, 2-methoxyaniline monomer contained in the interior of micelles would diffuse to the surface, resulting in the formation of hollow microspheres (Scheme 2C). As the pH drops during the initial stages of the oxidative polymerization, the sulphonic acid groups of NSA will become partially protonated while being incorporated within the P2MA structure. The flux of water and water-soluble components into the interior of the growing nanospheres probably leads to the formation of openings or holes on the surfaces, visible for many of the hollow spheres.

#### Electrochemical property

The cyclic voltammograms of P2MA-NSA/GCE in 0.1 M HCl with scan rates of 10, 20, 30, 40, 50, 60, 70, 80, 90 and 100 mVs<sup>-1</sup> are shown in Fig. 5. From the Fig. 5, it can be seen that the peak potentials and corresponding currents vary with the change in scan rates value. This indicates that the P2MA-NSA hollow spheres are electroactive and the electron transfer processes are coupled to a diffusion process namely, charge transportation along the polymeric nanostructures. Further, Fig. 5 shows 2 pairs of redox peaks. The first redox peak (I/IV) represents poly(2-methoxyaniline) radical cation/ poly(2-methoxyaniline) base and the second redox peak (II/III) corresponds to poly(2-methoxyaniline) base/ poly(2-methoxyaniline) radical [20] cation

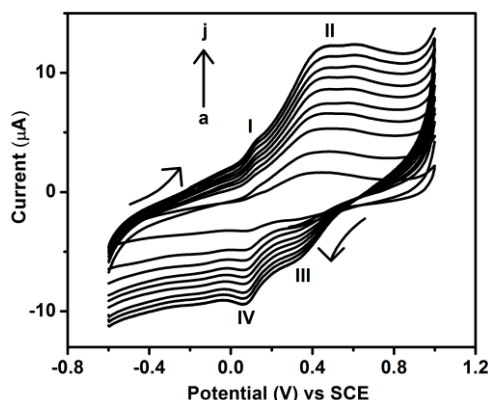


**Fig. 5:** Cyclic voltammograms of P2MA-NSA/GCE in 0.1 HCl solution at the scan rate of (a) 10, (b) 20, (c) 30, (d) 40, (e) 50, (f) 60, (g) 70, (h) 80, (i) 90 and (j) 100 mVs<sup>-1</sup>.

#### Electrochemical sensing property

Fig. 6 shows the cyclic voltammograms (CVs) of 0.1 mM UA at bare and P2MA-NSA/GCE at scan rate 50 mVs<sup>-1</sup>. The electrochemical oxidation of UA proceeds in a 2e<sup>-</sup>, 2H<sup>+</sup> process to lead to an unstable diimine species which is then attacked by water molecules in a step-wise fashion to be converted into an imine-alcohol and then uric acid-4,5 diol. The uric acid-4,5 diol compound produced is unstable and decomposes to various products depending on the solution pH [21]. At P2MA-NSA/GCE, well defined oxidation wave of UA with enhanced peak current was obtained. This electrocatalytic effect was attributed to the larger available surface area and good conducting nature of P2MA-NSA microspheres [22]. Based on the previous report [11, 21] the possible electrochemical oxidation of UA at P2MA-NSA/GCE is explained.

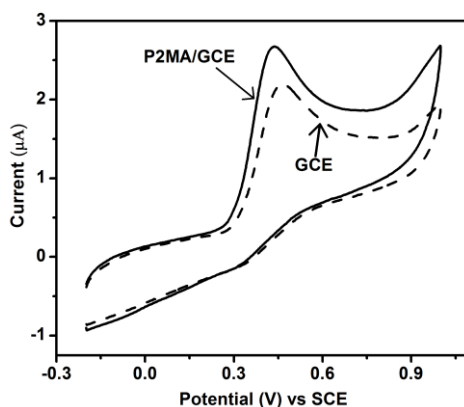


Fig. 6: Cyclic voltammogram of bare and P2MA-NSA/GCE in presence of 0.1 mM UA in 0.1 M phosphate buffer solution (pH = 7.4).

Fig. 7 shows the effect of scan rate on P2MA-NSA/GCE in presence of 0.1 mM UA. The shift towards higher values of the oxidation peak potential with increasing scan rates can be observed, indicating a kinetic limitation in the reaction between redox sites of P2MA-NSA/GCE and UA. However, the anodic peak currents for UA at P2MA-NSA/GCE are linearly related to the scan rate in the range 10-100 mVs<sup>-1</sup>, which indicated that the electron transfer reaction was controlled by diffusion process [23]. Since chronoamperometry is more sensitive than cyclic voltammetry, CA was used for detection of UA by P2MA-NSA/GCE is done. According to the potential dependence of the UA electrocatalytic oxidation at stirring conditions, the optimum electrode potential was selected at 0.47 V versus SCE for chronoamperometric measurements in order to obtain sensitivity. Fig. 8 shows the chronoamperometric response of P2MA-NSA/GCE upon the addition of 0.2 mL of 0.1 mM UA. A successive addition of UA to continuously stirred 0.1 M PBS (pH = 7.4) produces a significant increase in electrocatalytic oxidation peak current. The calibration plot of the P2MA-NSA/GCE is shown as the inset in Fig. 8. The linear chronoamperometric response is in the range from 6.6 µM to 62.5 µM ( $R^2 = 0.9977$ ) corresponding with a sensitivity of 0.003 µAµM<sup>-1</sup>, shows that the P2MA-NSA/GCE is sensitive towards UA.

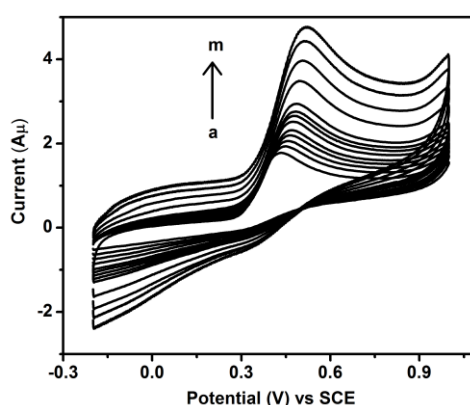


Fig. 7: Cyclic voltammograms of P2MA-NSA/GCE in presence of 0.1 mM UA in 0.1 M phosphate buffer solution (pH = 7.4). at the scan rate of (a) 20, (b) 30, (c) 40, (d) 50, (e) 60, (f) 70, (g) 80, (h) 90, (i), 100, (j) 150, (k) 200, (l) 250 and (m) 300 mVs<sup>-1</sup>

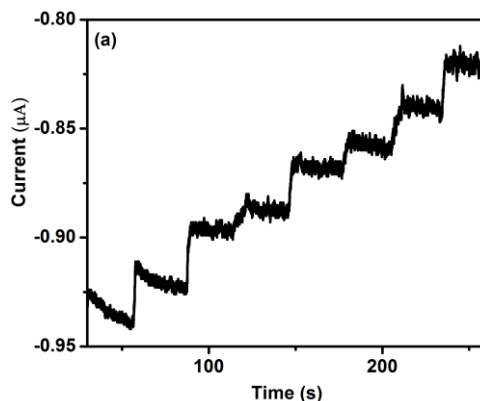


Fig. 8: Chronoamperometric responses of P2MA-NSA/GCE for the successive additions of 0.2 mL of 0.1 mM UA to 30 mL of 0.1 M PBS. Applied potential is 0.47 V.

Based on the above results, the catalytic reaction occurred between P2MA-NSA/GCE with UA. The catalytic reaction facilitates electron transfer between UA and P2MA-NSA/GCE, as a result the electrochemical oxidation of UA becomes easier. The reason for this is that the P2MA-NSA microspheres can act as a promoter to increase the rate of electron transfer, lower the overpotential of UA at the bare electrode, and the anodic peak shifts less positive potential. Thus, it is clear that P2MA-NSA/GCE can be successfully used for the determination of biomolecules.

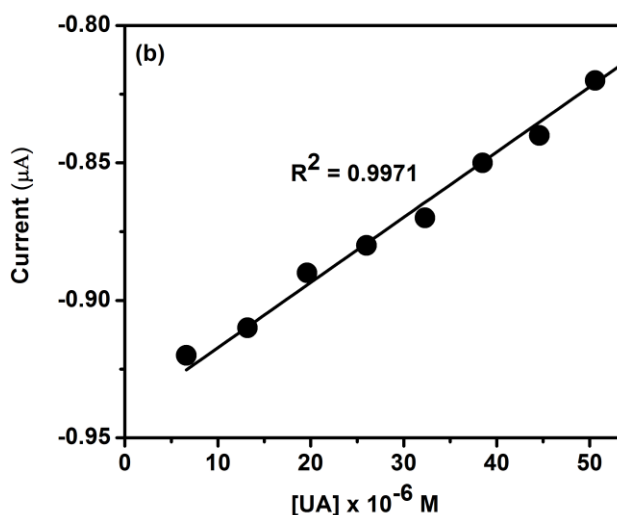


Fig. 9: Plot of UA anodic peak current versus concentration of UA.

#### IV. CONCLUSION

The P2MA-NSA microspheres were prepared by oxidative polymerization method using potassium persulphate as an oxidant. The FT-IR and Raman spectrum confirms the structure of the P2MA-NSA. It also confirms that NSA is incorporated within the P2MA microspheres. UV-Visible spectrum of P2MA-NSA microspheres predict that the introduction of -OCH<sub>3</sub> group in the aromatic ring of polymer produces a blue shift. The SEM micrograph of P2MA-NSA shows that the particles are hollow microspheres with the diameter in range of 1-2 μm. Cyclic voltammetry showed that the electrochemical properties of NSA doped P2MA microspheres which are closely resembled to the properties of conventional P2MA nanostructures. Further, the electrochemical sensing experiments showed that the prepared P2MA-NSA microspheres will be a good candidate in the field of biosensor.

**International Journal of Innovative Research in Science, Engineering and Technology**

*An ISO 3297: 2007 Certified Organization*

*Volume 4, Special Issue 1, February 2015*

**THIRD NATIONAL CONFERENCE ON ADVANCES IN CHEMISTRY (NCAC – 2015)**

**On 18<sup>th</sup> February 2015**

**Organized by**

**Department of Chemistry, Easwari Engineering College (SRM Group of Institutions), Chennai-600089, India.**

**ACKNOWLEDGMENTS**

One of the authors (RS) wish to thank Council for Scientific Industrial Research (CSIR), Government of India for the financial assistance in the form of Senior Research Fellowship. Authors thank to National Centre for Nanoscience and Nanotechnology (NCNSNT), University of Madras for providing Raman facility.

**REFERENCES**

1. E.I. Iwuoha, S.E. Mavundla, V.S. Somerset, L.F. Petrik, P. Baker, *Microchim. Acta* 155 (2006) 453.
2. V. Bavastrello, E. Strura, S. Carrara, V. Erokhin, C. Nicolini, *Sens. Actuators* 98 (2004) 247.
3. J. Huang, R.B. Kaner, *J. Am. Chem. Soc.* 126 (2004) 851.
4. P. Yin, P.A. Kilmartin, *Curr. Appl. Phys.* 4 (2004) 141.
5. L. Huang, T. Wen, A. Gopalan, *Mater. Lett.* 57 (2003) 1765.
6. J.E. Fromer, R.R. Chance. "Encyclopedia of Polymer Science and Engineering", Wiley, New York, 1986, pp.462.
7. X. Feng, C. Mao, G. Yang, W. Hou, J.J. Zhu, *Langmuir* 22 (2006) 4384.
8. J. Yang, M.S. Burkinshaw, J. Zhou, P.A. Monkman, P.J. Brown, *Adv. Mater.* 15 (2003) 1081.
9. S.E. Mavundla, G.F. Malgas, P. Baker, E.I. Iwuoha, *Electroanalysis* 20 (2008) 2347.
10. H. Yan, H.J. Wang, S. Adisasmito, N. Toshima, *Bull. Chem. Soc. Jpn.* 69 (1996) 2395.
11. R. Suresh, R. Prabu, A. Vijayaraj, K. Giribabu, R. Manigandan, A. Stephen, V. Narayanan, *Bull. Korean Chem. Soc.* 33 (2012) 1919.
12. R. Suresh, R. Prabu, A. Vijayaraj, K. Giribabu, A. Stephen, V. Narayanan, *Mater. Chem. Phys.* 134 (2012) 590.
13. L. Zhang, H. Peng, C. Fang, P.A. Kilmartin, J. Travas sejdic, *Nanotechnology* 18 (2007) 115607.
14. H. Kunglin, S.A. Chen, *Macromolecules* 33 (2000) 8117.
15. Z. Ping, *J. Chem. Soc., Faraday Trans.* 92 (1996) 3063.
16. M.V. Kulkarni, A.K. Viswanath, *Eur. Polym. J.* 40 (2004) 379.
17. J.M. Ginder, A.J. Epstein, *Phys. Rev.* B41 (1990) 10674.
18. P. Ghosh, S.K. Siddhanta, *J. Polym. Sci., Part A: Polym. Chem.* 37 (1999) 3243.
19. C. Luo, H. Peng, L. Zhang, G.L. Lu, Y. Wang, J.T. Sejdic, *Macromolecules* 44 (2011) 6899.
20. C.J. Weng, P.H. Hsu, S.C. Hsu, C.H. Chang, W.I. Hung, P.S. Wu, J.M. Yeh, *J. Mater. Chem. B* 1 (2013) 4983.
21. P.R. Roy, T. Okajima, T. Ohsaka, *J. Electroanal. Chem.* 561 (2004) 75.
22. S. Reddy, B.E. Kumara Swamy, U.Chandra, B.S. Sherigara, H. Jayadevappa, *Int. J. Electrochem. Sci.* 5 (2010) 10.
23. K. Giribabu, R. Suresh, R. Manigandan, S. Munusamy, S. Praveen Kumar, S. Muthamizh, V. Narayanan, *Analyst* 138 (2013) 5811.